P H Y S I C A L   R E V I E W   L E T T E R S

Exact Characterization of $O(n)$ Tricriticality in Two Dimensions

Wenan Guo,[1] Bernard Nienhuis,[2] and Henk W. J. Blöte[3,4]

[1]*Physics Department, Beijing Normal University, Beijing 100875, People's Republic of China*
[2]*Instituut voor Theoretische Fysica, Universiteit van Amsterdam, Valckenierstraat 65, The Netherlands*
[3]*Faculty of Applied Sciences, Delft University of Technology, P.O. Box 5046, 2600 GA Delft, The Netherlands*
[4]*Instituut Lorentz, Leiden University, P.O. Box 9506, 2300 RA Leiden, The Netherlands*
(Received 10 November 2005; published 1 February 2006)

We propose exact expressions for the conformal anomaly and for three critical exponents of the tricritical $O(n)$ loop model as a function of n in the range $-2 \leq n \leq 3/2$. These findings are based on an analogy with known relations between Potts and $O(n)$ models and on an exact solution of a "tri-tricritical" Potts model described in the literature. We verify the exact expressions for the tricritical $O(n)$ model by means of a finite-size scaling analysis based on numerical transfer-matrix calculations.

While exact results exist for a rich collection of universality classes of two-dimensional phase transitions, including q-state Potts criticality and tricriticality, and $O(n)$ criticality, such results are still absent for the tricritical $O(n)$ model, except for isolated points at $n = 0$ and 1. The purpose of the present work is to fill in this gap and to provide exact formulas for the conformal anomaly and the main scaling dimensions of the tricritical $O(n)$ model as a function of n. These results are not rigorous in the mathematical sense, but they may still be assumed to be exactly true, as we shall argue below.

The $O(n)$ model is defined in terms of n-component spins on a lattice, with an isotropic pair coupling of the form $E_{ij} = \epsilon(\vec{S}_i \cdot \vec{S}_j)$, where i and j denote two neighboring lattice sites and ϵ is a function. This model can be represented by a graph expansion [1], in which n assumes the role of a continuous parameter. For this purpose, it is especially useful to choose the model on the honeycomb lattice, and the function ϵ as $\epsilon(p) \equiv -\log(1 + xp)$, where x is a measure of the inverse temperature. Then the graph expansion reduces to a gas of nonintersecting and nonoverlapping loops on the honeycomb lattice [2]. This loop gas representation enables further mappings on the Kagomé 6-vertex model and the Coulomb gas, and has therefore played a crucial role as a step in the derivation of exact results for the honeycomb $O(n)$ model [3,4].

Just as for the Potts model, tricriticality can be induced by introducing a sufficient number of vacancies. This was already known [5,6] for the case $n = 0$ which describes the collapse of a polymer at the so-called theta point, induced by attractive interactions between the polymer segments, and for the Ising case $n = 1$ [7,8] where the existing results for the tricritical $q = 2$ Potts model apply [9]. For the $O(n)$ loop model, the existence of tricritical points was further confirmed by transfer-matrix analyses for a range of values of n [10,11]. Whereas this work yielded reasonably accurate values for some universal parameters, no exact formulas were found for these parameters as a function of n.

Recently, Janke and Schakel [12] reconsidered the tricritical $O(n)$ model and postulated that the conformal classification in terms of the Kac formula [13,14] of the magnetic exponent, which is known to be $X_h = X_{m/2,m/2}$ [as given below in Eq. (8)] for $n = 0$ and 1, generalizes to other n.

In order to find the "missing link," which is the relation between n and the conformal anomaly c, a clue is provided by the observation that a *critical $O(n)$* model corresponds with a *tricritical $q = n^2$-state* Potts model [3]. It would thus be interesting to bring the tricritical Potts model into an even higher critical state. This appears to be possible [15,16] by the simultaneous introduction of vacancies and their dual counterparts, four-spin couplings, into the Potts model. The equivalent loop model on the surrounding lattice then appears to have a parameter subspace where the Yang-Baxter equations are solvable [15]. Out of four branches of solutions parametrized by q, one was identified as a branch of tri-tricritical Potts transitions [15,16]. The conformal anomaly and exponents of this model are found as a function of q by using an alternative representation as a Temperley-Lieb model [15].

Since the equivalent loop model has loop weight $\sqrt{q}$, it seems an appealing possibility that the universal properties of the q-state tri-tricritical Potts model match those of the tricritical $O(n = \sqrt{q})$ loop model. The conformal anomaly derived in Ref. [15] is, expressed in $n = \sqrt{q}$, determined by the following equations:

$$c = 1 - \frac{6}{m(m+1)}, \qquad 2\cos\frac{\pi}{m+1} = \Delta, \qquad \Delta - \frac{1}{\Delta} = n. \tag{1}$$

Furthermore, Ref. [15] yielded scaling dimensions of which we quote three as

$$X_j = (k_j^2 - 1)/[2m(m+1)], \tag{2}$$

where we introduced an index $j = 1, 2,$ or 3, and k_j is given

by $\Delta_j = 2\cos[k_j\pi/(m+1)]$, with $\Delta_1 = 1/\Delta$, $\Delta_2 = -1/\Delta$, and $\Delta_3 = -\Delta$.

In order to verify the relation with the tri-tricritical Potts model, we employ transfer-matrix calculations for the loop model on the honeycomb lattice with vacancies. These are introduced as face variables located on the elementary hexagons. They have two possible states: vacant (weight v) or occupied (weight $1 - v$). Furthermore, there is an n-component vector spin $\vec{S}_i$ on each vertex i that is surrounded by three occupied hexagons. The one-spin weight distribution is isotropic and normalized such that $\int d\vec{S} = 1$ and $\int d\vec{S} \, \vec{S} \cdot \vec{S} = n$. The partition function given by [3] thus generalizes to

$$Z = \sum_{\mathcal{L}} v^{N_v}(1 - v)^{N - N_v} \int \prod_{i|\mathcal{L}} d\vec{S}_i \prod_{\langle ij \rangle}(1 + w\vec{S}_i \cdot \vec{S}_j), \quad (3)$$

where the sum is on all configuration variables: $\mathcal{L}$ is a subset of the dual lattice and represents the occupied faces of the honeycomb lattice. The product over $i|\mathcal{L}$ includes all vertices except those of the vacant hexagons, N_v is the number of vacant faces, N is the total number of faces, w controls the strength of the spin-spin coupling, and $\langle ij \rangle$ denotes all nearest-neighbor spin pairs. The mapping on a loop model proceeds along the same lines as in Ref. [2] and leads to the following partition sum:

$$Z = \sum_{\mathcal{L}} \sum_{\mathcal{G}|\mathcal{L}} v^{N_v}(1 - v)^{N - N_v} w^{N_w} n^{N_l}, \quad (4)$$

where the first sum is on all possible configurations $\mathcal{L}$ of occupied faces, and the second one over all configurations $\mathcal{G}$ of closed loops on the honeycomb lattice that avoid empty faces; w is the bond weight, N_w is the number of bonds (or, equivalently, vertices) on $\mathcal{G}$, and N_l the number of loops.

The transfer matrix is constructed for a model wrapped on a cylinder, whose axis is parallel to one of the lattice edge directions. The unit of length is defined as the small diameter of an elementary hexagon. The transfer matrix keeps track of the change of the number of loops, vacancies, and visited vertices when a new layer of sites is added to the cylinder. Its largest eigenvalue determines finite-size data for the free energy density, from which the conformal anomaly can be estimated [17]. Three more eigenvalues λ_i were calculated. These determine three correlation lengths and allow finite-size estimates $X_i(v, w, L)$ of the corresponding scaling dimensions X_i [18]. The temperature dimension X_t was estimated from the second eigenvalue of the transfer matrix, and the magnetic dimension X_h from a modified transfer matrix with a single loop segment running in the length direction of the cylinder. The "interface" exponent X_m was estimated by inserting a column with bond weights of the opposite sign. Further details about the transfer-matrix technique are given in Refs. [10,11,19].

We parametrize the vicinity of the tricritical fixed point by two relevant temperaturelike fields t_1 and t_2 and by an irrelevant field u. The associated exponents are y_{t_1}, y_{t_2}, and y_u, respectively, with $y_{t_1} > y_{t_2}$.

The tricritical point is estimated by simultaneously solving the unknowns v and w in the two equations

$$X_i(v, w, L) = X_i(v, w, L - 1) = X_i(v, w, L - 2), \quad (5)$$

where the functions X_i ($i = h, t, m$) are provided by the transfer-matrix algorithm. Expansion of the finite-size-scaling function in the vicinity of the tricritical point yields that the solution $v(L)$ of Eq. (5) converges to the tricritical value $v^{(\text{tri})}$ of v as

$$v(L) = v^{(\text{tri})} + aL^{y_u - y_{t_2}} + \cdots, \quad (6)$$

where a is an unknown constant; $w(v, L)$ similarly converges to the tricritical value $w^{(\text{tri})}$. The values $X_i(L)$ taken at the solutions of Eq. (5) converge to the tricritical scaling dimension X_i as

$$X_i(L) = X_i + buL^{y_u} + \cdots, \quad (7)$$

where b is another unknown constant. We applied this procedure for both $X_i = X_h$ and $X_i = X_m$ to locate the tricritical points and to estimate the tricritical exponents from Eq. (7). These calculations were performed along the same lines as in Ref. [11], but here we use larger finite sizes up to $L = 14$, and moreover, we include several values for $-2 \leq n < 0$. The results for the tricritical points are listed in Table I, together with the estimated error margins.

The analyses using X_h and X_m generated consistent results and allowed us to check the numerical uncertainties.

TABLE I. Tricritical points as determined from the transfer-matrix calculations described in the text. The estimated numerical uncertainty in the last decimal place is shown in parentheses.

n	v	w
−2.0	0.3503(1)	0.8156(1)
−1.75	0.3649(1)	0.8330(1)
−1.50	0.380 081 4(1)	0.852 082(1)
−1.25	0.397 935 2(1)	0.872 640 4(1)
−1.00	0.416 356 8(3)	0.894 926 8(1)
−0.75	0.436 008 8(1)	0.918 961 7(2)
−0.50	0.456 683 4(2)	0.944 610 0(2)
−0.25	0.478 147 5(2)	0.971 742 8(2)
0	1/2	1
0.25	0.521 805(1)	1.028 950(1)
0.50	0.543 13(1)	1.058 12(1)
0.75	0.563 61(2)	1.087 08(2)
1.00	0.5830(1)	1.1155(1)
1.25	0.6010(1)	1.1429(1)
1.50	0.6175(1)	1.1688(1)
1.75	0.6321(1)	1.1928(1)
2.00	0.6452(1)	1.2145(1)

We also obtained finite-size estimates of X_t at the tricritical points thus calculated, and extrapolated these data. The results for the conformal anomaly and the three exponents are listed in Table II, together with the estimated error margins.

A comparison of the numerical results for the conformal anomaly with Eq. (1), as given in Table II, strongly supports the classification of the tricritical $O(n)$ model as proposed for $n \leq 3/2$. Our numerical results for X_t agree with X_2 in Eq. (2); those for X_m agree with X_1. Using the value of the conformal anomaly and m as a function n, we confirm that the numerical results for the magnetic scaling dimension agree with the entry $(i = m/2, j = m/2)$ in the Kac formula:

$$X_{i,j} = \frac{[i(m+1) - jm]^2 - 1}{2m(m+1)}. \tag{8}$$

The $n > 0$ results correspond with branch 1 as defined in Ref. [15], and those for $n < 0$ with branch 2. The numerical results and theoretical values of the conformal anomaly and the dimensions are shown as a function of n in Figs. 1 and 2.

The expressions for X_1 and X_2 in Eq. (2) are not reproduced by entries in the Kac table, at least not with index pairs that are linear in m. This made it difficult to conjecture the exact values of X_m and X_t from numerical data alone, even if supported by data for c. This problem did not apply to X_h, which appears in the Kac table.

Remarkably, the Potts tri-tricritical branch ends at $q = 9/4$. For $q > 9/4$ the model is no longer critical and the transition probably turns first order [15,16]. The equivalence $q = n^2$ thus yields the result that the tricritical $O(n)$ branch ends at $n = 3/2$, possibly with a discontinuous transition for $n > 3/2$. At first sight, the numerical results for $3/2 < n \leq 2$ may not seem suggestive of a discontinuous transition, and allow only a very weak discontinuity. But it is clear from Tables I and II that the estimated errors tend to increase with n for $n \gtrsim 3/2$, as a result of deteriorating finite-size convergence. This is consistent with the possibility that an operator becomes marginal at $n = 3/2$, in line with $c = 1$ (see Table II). Therefore, one may expect similar phenomena as for the $q > 4$ Potts model, where the marginal operator leads to misleadingly slow finite-size convergence which obscures the weak first-order character in a range of q near 4.

The results presented above apply to the nonintersecting loop model. Loop intersections are irrelevant in the critical $O(n)$ model, but they are relevant in the low-temperature phase [20]. While the possible relevance of such intersections could modify the universal behavior, this appears not to be the case for the $n = 1$ tricritical $O(n)$ loop model, since its exponents agree with those of the corresponding spin model.
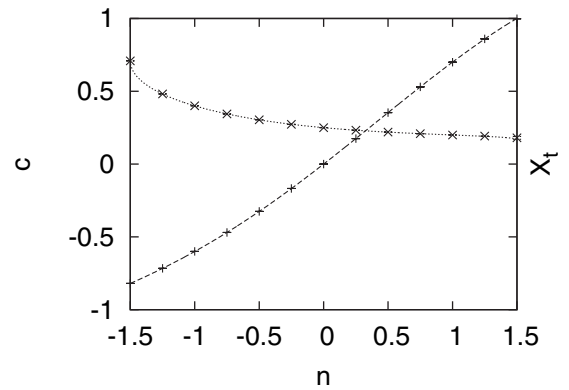
TABLE II. Conformal anomaly and tricritical exponents as determined from the transfer-matrix calculations described in the text. Estimated error margins in the last decimal place are given in parentheses. The numerical results are indicated by "(num)." For comparison, we include theoretical values obtained from Eqs. (1), (2), and (8). For $n < -3/2$, the temperature exponent X_t becomes complex.

n	c (num)	c (exact)	X_m (num)	X_m (exact)
-2.0	$-0.9914(2)$	-0.9915599	$-0.202(1)$	-0.2017990
-1.75	$-0.9108(2)$	-0.9109986	$-0.1765(2)$	-0.1769723
-1.50	$-0.8196(2)$	-0.8197365	$-0.15166(3)$	-0.1516447
-1.25	$-0.7164(1)$	-0.7164556	$-0.12596(3)$	-0.1259301
-1.00	$-0.6000(1)$	$-6/10$	$-0.10001(2)$	$-1/10$
-0.75	$-0.46962(1)$	-0.4696195	$-0.07410(1)$	-0.0740955
-0.50	$-0.32528(1)$	-0.3252829	$-0.04853(1)$	-0.0485319
-0.25	$-0.16799(1)$	-0.1679953	$-0.023691(1)$	-0.0236917
0	0	0	0	0
0.25	$0.17526(1)$	0.1752630	$0.022111(1)$	0.0221110
0.50	$0.35348(1)$	0.3534792	$0.04224(1)$	0.0422357
0.75	$0.52994(1)$	0.5299489	$0.05999(1)$	0.0600004
1.00	$0.70000(1)$	$7/10$	$0.0749(1)$	$3/40$
1.25	$0.860(1)$	0.8589769	$0.0867(2)$	0.0865052
1.50	$1.001(2)$	1	$0.094(5)$	0.0880192
1.75	$1.04(4)$		$0.098(5)$	
2.00	$1.05(2)$		$0.10(1)$	
n	X_t (num)	X_t (exact)	X_h (num)	X_h (exact)
-2.0	$\cdots$	$\cdots$	$-0.094(1)$	-0.0951627
-1.75	$\cdots$	$\cdots$	$-0.087(1)$	-0.0876431
-1.50	$0.709(1)$	0.7097847	$-0.0792(1)$	-0.0790909
-1.25	$0.4817(2)$	0.4814739	$-0.0694(1)$	-0.0693653
-1.00	$0.4000(2)$	$2/5$	$-0.0584(1)$	$-7/120$
-0.75	$0.3445(2)$	0.3446681	$-0.04593(3)$	-0.0458895
-0.50	$0.30390(2)$	0.3039309	$-0.03199(1)$	-0.0319828
-0.25	$0.273220(1)$	0.2732199	$-0.016645(1)$	-0.0166435
0.00	$1/4$	$1/4$	0	0
0.25	$0.232500(1)$	0.2324957	$0.017731(1)$	0.01772952
0.50	$0.2193(1)$	0.2192386	$0.03628(1)$	0.03627658
0.75	$0.2090(2)$	0.2088741	$0.05539(1)$	0.05539746
1.00	$0.2000(1)$	$1/5$	$0.07500(2)$	$3/40$
1.25	$0.193(1)$	0.1906800	$0.0950(2)$	0.09549714
1.50	$0.180(5)$	0.1684499	$0.12(1)$	$1/8$
1.75	$0.183(10)$		$0.13(1)$	
2.00	$0.184(10)$		$0.15(2)$	

FIG. 1.   Conformal anomaly ($+$) and temperature exponent ($\times$) of the tricritical $O(n)$ model vs n. The data points show the numerical data, the curves the theoretical predictions.
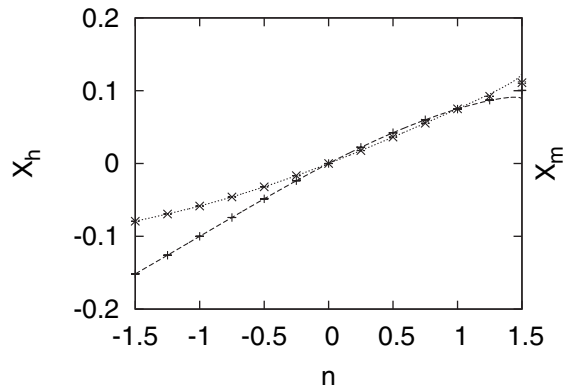
FIG. 2.   Scaling dimensions X_h (×) and X_m (+) of the tricritical $O(n)$ model vs n. The data points show the numerical data, the curves the theoretical predictions.

The scenario sketched above indicates that the critical and tricritical $O(n)$ branches are *not connected*, and does not identify the loop gases corresponding to the tricritical $O(n)$ model and the critical Potts model, such as was recently suggested [12].

[1] H. E. Stanley, Phys. Rev. Lett. **20**, 589 (1968).
[2] E. Domany, D. Mukamel, B. Nienhuis, and A. Schwimmer, Nucl. Phys. **B190**, 279 (1981).
[3] B. Nienhuis, Phys. Rev. Lett. **49**, 1062 (1982); J. Stat. Phys. **34**, 731 (1984).
[4] R. J. Baxter, J. Phys. A **19**, 2821 (1986); **20**, 5241 (1987).
[5] B. Duplantier and H. Saleur, Phys. Rev. Lett. **59**, 539 (1987).
[6] H. W. J. Blöte, M. T. Batchelor, and B. Nienhuis, Physica (Amsterdam) **251A**, 95 (1998).
[7] M. Blume, Phys. Rev. **141**, 517 (1966).
[8] H. W. Capel, Physica (Amsterdam) **32A**, 966 (1966); Phys. Lett. **23**, 327 (1966).
[9] B. Nienhuis, *Phase Transitions and Critical Phenomena*, edited by C. Domb and J. L. Lebowitz (Academic Press, London, 1987), Vol. 11.
[10] W.-A. Guo, H. W. J. Blöte, and B. Nienhuis, Int. J. Mod. Phys. C **10**, 291 (1999).
[11] W.-A. Guo, H. W. J. Blöte, and Y.-Y. Liu, Commun. Theor. Phys. **41**, 911 (2004).
[12] W. Janke and A. M. J. Schakel, Phys. Rev. Lett. **95**, 135702 (2005).
[13] D. Friedan, Z. Qiu, and S. Shenker, Phys. Rev. Lett. **52**, 1575 (1984).
[14] V. G. Kac, in *Group Theoretical Methods in Physics*, edited by W. Beiglbock and A. Bohm, Lecture Notes in Physics Vol. 94 (Springer, New York, 1979), p. 441.
[15] B. Nienhuis, S. O. Warnaar, and H. W. J. Blöte, J. Phys. A **26**, 477 (1993).
[16] Y. M. M. Knops, H. W. J. Blöte, and B. Nienhuis, J. Phys. A **26**, 495 (1993).
[17] H. W. J. Blöte, J. L. Cardy, and M. P. Nightingale, Phys. Rev. Lett. **56**, 742 (1986).
[18] J. L. Cardy, J. Phys. A **17**, L385 (1984).
[19] H. W. J. Blöte and B. Nienhuis, J. Phys. A **22**, 1415 (1989).
[20] J. L. Jacobsen, N. Read, and H. Saleur, Phys. Rev. Lett. **90**, 090601 (2003).